THE JOURNAL OF BIOLOGICAL CHEMISTRY VOL. 289, NO. 28, pp. 19269–19275, July 11, 2014

Secreted Histidyl-tRNA Synthetase Splice Variants Elaborate Major Epitopes for Autoantibodies in Inflammatory Myositis*[S]

Received for publication, April 5, 2014, and in revised form, May 30, 2014
Published, JBC Papers in Press, June 4, 2014, DOI 10.1074/jbc.C114.571026

Jie J. Zhou[‡§], Feng Wang[‡§], Zhiwen Xu[‡§], Wing-Sze Lo[‡§], Ching-Fun Lau[‡§], Kyle P. Chiang[¶], Leslie A. Nangle[¶], Melissa A. Ashlock[¶], John D. Mendlein[¶], Xiang-Lei Yang[‡‖], Mingjie Zhang[‡], and Paul Schimmel[‡‖‡‡1]**

*From the [‡]IAS HKUST-Scripps R&D Laboratory, Institute for Advanced Study, and **Division of Life Science, State Key Laboratory of Molecular Neuroscience, Hong Kong University of Science and Technology, Clear Water Bay, Kowloon, Hong Kong, China, [§]Pangu BioPharma, Hong Kong, China, [¶]aTyr Pharma, San Diego, California 92121, [‖]The Scripps Research Institute, La Jolla, California 92037, and [‡‡]Scripps Florida, Jupiter, Florida 33458*

Background: Autoantibodies (anti-Jo-1) to cytoplasmic histidyl-tRNA synthetase (HisRS) are associated with inflammatory myositis.
Results: HisRS and two splice variants (SVs) cross-react with anti-Jo-1 antibodies and are secreted; at least one SV transcript is up-regulated in dermatomyositis.
Conclusion: Secreted HisRS SVs contain major epitopes of anti-Jo-1 autoantibodies.
Significance: Secreted HisRS and its SVs share epitopes for potential extracellular anti-Jo-1 antibody binding.

Inflammatory and debilitating myositis and interstitial lung disease are commonly associated with autoantibodies (anti-Jo-1 antibodies) to cytoplasmic histidyl-tRNA synthetase (HisRS). Anti-Jo-1 antibodies from different disease-afflicted patients react mostly with spatially separated epitopes in the three-dimensional structure of human HisRS. We noted that two HisRS splice variants (SVs) include these spatially separated regions, but each SV lacks the HisRS catalytic domain. Despite the large deletions, the two SVs cross-react with a substantial population of anti-Jo-1 antibodies from myositis patients. Moreover, expression of at least one of the SVs is up-regulated in dermatomyositis patients, and cell-based experiments show that both SVs and HisRS can be secreted. We suggest that, in patients with inflammatory myositis, anti-Jo-1 antibodies may have extracellular activity.

Idiopathic inflammatory myositis (IIM)[2] is an autoimmune disease that is strongly associated with autoantibodies and is frequently associated with interstitial lung disease (ILD) (1). Myositis-specific antibodies (MSAs) and myositis-associated antibodies define two distinct groups (2). MSAs are directed against histidyl-, threonyl-, alanyl-, glycyl-, isoleucyl-, and asparaginyl-tRNA synthetases. Interestingly, in any single patient, these MSAs are mutually exclusive (1).

Among the myositis-specific anti-aaRS Abs, those directed against cytoplasmic histidyl-tRNA synthetase (HisRS) are the most common (3) and were first described >30 years ago (4). Approximately 25–30% of patients with dermatomyositis (DM) or polymyositis have anti-HisRS Abs (3). In contrast, autoantibodies directed against the other five aaRSs collectively constitute a much smaller percentage (3–5). Anti-HisRS Abs, which were historically designated as anti-Jo-1 Abs, bind to sites that are spread across the entire protein and include both linear and conformational epitopes (6, 7).

Among the various epitopes, the N-terminal portion of HisRS is especially prominent (6–8). In ELISA, recombinant HisRS(1–60) (constituting the first 60 amino acids (aa)) reacted with anti-Jo-1 Abs, whereas a truncated HisRS lacking the first 60 aa failed to react (7). Interestingly, the first 60 aa of HisRS are encoded by the first two exons of the mRNA of *HARS* and are absent from HisRSs of prokaryotes and lower eukaryotes. As expected, anti-Jo-1 Abs do not react with *Escherichia coli* HisRS (9). According to our structural analysis, this small domain (designated as a WHEP domain) forms a helical coiled-coil structure (9). Other work showed that HisRS(1–48) induced migration of $CD4^+$ and $CD8^+$ lymphocytes, IL-2-activated monocytes, and immature dendritic cells. In contrast, HisRS(61–509), which lacks the first 60 aa, failed to stimulate these inflammation-related cell migration events (8). Other *in vivo* studies in mice suggest that HisRS has an etiological relationship to the disease (10).

Despite the wealth of data on the association of HisRS with anti-Jo-1 Ab in IIM/ILD, the cross-reactivity of splice variants (SVs) with anti-Jo-1 Abs is undefined. In this in mind, we previously identified HisRSΔCD, a natural HisRS SV that has an internal deletion that ablates the entire catalytic domain (CD) and joins the N-terminal WHEP domain (1–60 residues) to the C-terminal anticodon-binding domain (ABD) (9). The result is a change in both quaternary and tertiary structures. Thus, HisRSΔCD is a monomer (HisRS is a homodimer) shaped like a dumbbell-like structure, where a flexible linker joins its two

* This work was supported, in whole or in part, by National Institutes of Health Grant CA92577 from NCI and Grant GM88278. This work was also supported by Innovation and Technology Fund of Hong Kong Grants UIM181, UIM192, and UIM199; aTyr Pharma; and an NFCR Fellowship (to the Scripps Laboratory for tRNA synthetase research) from the National Foundation for Cancer Research. Professors Mingjie Zhang, Xiang-Lei Yang, and Paul Schimmel are financially benefited by aTyr Pharma in the form of compensation, stock ownership, or both.
[S] This article contains supplemental Fig. S1.
[1] To whom correspondence should be addressed: IAS HKUST-Scripps R&D Laboratory, Institute for Advanced Study, HKUST, Clear Water Bay, Kowloon, Hong Kong. Tel.: 852-2358-5022; Fax: 852–2719-8158; E-mail: schimmel@scripps.edu.

[2] The abbreviations used are: IIM, idiopathic inflammatory myositis; ILD, interstitial lung disease; MSA, myositis-specific antibody; aaRS, aminoacyl-tRNA synthetase; HisRS, histidyl-tRNA synthetase; DM, dermatomyositis; aa, amino acid(s); SV, splice variant; CD, catalytic domain; ABD, anticodon-binding domain; qPCR, quantitative PCR; TCL, total cell lysate; LDH, lactose dehydrogenase; EST, expressed sequence tag; HKG, house-keeping gene.

domains and the ABD has an altered conformation. Although the epitopes were not mapped, HisRSΔCD reacted with anti-Jo-1 Abs from patient sera (9).

Interestingly, we identified another novel HisRS SV in muscle tissue, which we designated as $HisRS^{WHEP}$. This SV is composed solely of the first 60 aa of HisRS, which constitute the WHEP domain. It results from a splice event that introduces a stop codon from intron 2. With this discovery, we then set out to investigate whether transcripts for HisRSΔCD and $HisRS^{WHEP}$ are up-regulated in patients with IIM/ILD. In addition, we investigated recombinant forms of these variants and their constituent domains for their reaction with anti-Jo-1 Abs from patients. Our results demonstrate that both the expression and cross-reactivity of HisRSΔCD and of $HisRS^{WHEP}$ are associated with IIM and therefore support the possibility of extracellular anti-Jo-1 antibody binding to HisRS and its SVs.

EXPERIMENTAL PROCEDURES

PCR Identification of $HisRS^{WHEP}$—A human skeletal muscle cDNA library was used as a template (Clontech, Palo Alto, CA). PCR was performed with a pair of primers (FP1 (AGTGGACAGCCGGGATGGCAGAGC)/RP1 (GCTTGGAGTCTTCCCCATAC)), and the PCR product was validated by direct sequencing. A color-coded trace from sequencing is presented in supplemental Fig. S1.

Sample Preparation for Gene Expression Analysis—All human tissue poly(A)$^+$ RNAs were purchased from Clontech (catalog nos. 636170, 636591, 636128, 636105, 636113, 636119, 636121, 636101, 636118, 636146, 636125, 636162, and 636120). Muscle biopsies from DM patients were kindly provided by the Telethon Network of Genetic Biobanks (Milan, Italy). These samples consisted of 10 muscle biopsies from Caucasian DM patients (including five males and five females). The diagnosis was based on clinical manifestation and histology . Total RNA was isolated from muscle using a PARIS kit (Invitrogen) and was pooled together as the DM group. The control group was pooled total RNA from two healthy Caucasian subjects (including one male and one female; Clontech catalog no. 636534). First-strand cDNAs were synthesized as described previously (9).

Quantitative PCR and Data Analysis—Quantitative PCRs (qPCRs) were performed as described previously (9, 11). The qPCR primer sequences were as follows: qFP1, CACGGTGCAGAAGTCATTGAT; qRP1, TCCCCATACTTTCCCATCAGTG; qFP2, GTGCTCAAAACCCCCAAGTAGAG; qRP2, CACAGTGGCTCACGCCTGT; qFP3, ACCCCCAAGTAGAGACGAG; qRP3, TCTCGCGAACTGCCATCTG; qFP_{MXA}, ACCTGATGGCCTATCACCAG; and qRP_{MXA}, TTCAGGAGCCAGCTGTAGGT.

Detection of HisRS Proteins by Western Blot Analysis—Total cell lysates (TCLs) of monocytic THP-1 cells and human primary skeletal muscle cells (Cell Application, San Diego, CA) were prepared in 50 mM Tris buffer (pH 8.0) containing 1% Triton X-100 and 5 mM EDTA. TCLs (50 μg) were applied to electrophoresis and subsequent Western blot analysis with anti-HisRS mAb (Abnova, Walnut, CA).

Quantification of HisRS Levels in Monocytic THP-1 Cells—The cellular HisRS concentration was determined by standard sandwich ELISA (capture Ab, home-made anti-human HisRS mouse mAb; detection Ab, anti-human HisRS mAb (Abnova), biotinylated in-house). Recombinant human HisRS protein was used as the quantification standard (see below).

Protein Expression and Purification—The cDNAs encoding native human HisRS (aa 1–506), HisRSΔCD (aa 1–60 plus aa 405–506), $HisRS^{WHEP}$ (aa 1–60), CD (aa 54–398), and ABD (aa 406–506) were cloned into the pET21a vector with a C-terminal His_6 tag. From our experience, the C-terminal 3 aa (CIC, aa 507–509) reduce protein homogeneity; thus, these residues were removed in all constructs. The constructs were transformed into *E. coli* BL21(DE3) cells, and expressed proteins were purified by nickel-nitrilotriacetic acid affinity chromatography and further separated by size-exclusion chromatography in 1× PBS buffer with 1 mM DTT. The purity and homogeneity of each protein were checked by analytical size-exclusion chromatography and SDS-PAGE.

Depletion ELISA—Anti-Jo-1 autoantibody-positive patient sera were obtained from RDL Inc. (Los Angeles, CA). A 96-well enzyme immunoassay/radioimmunoassay plate (Corning, Corning, NY) was coated with 50 μl (2 μg/ml) of one of the recombinant proteins (see above) or BSA (as a control) in PBS buffer. After washing and blocking, patient sera containing anti-Jo-1 autoantibodies (in a dilution giving 25% of the maximum effect when applied to a HisRS-coated plate) were added and incubated overnight at 4 °C. After incubation, supernatant was applied to another plate (precoated with the respective recombinant protein) to check the depletion efficiency. The samples with a pre-depletion efficiency of >95% were applied to another plate coated with HisRS for indirect ELISA. The detection Ab was HRP-conjugated goat anti-human IgG (10 ng/well IgG; AbD Serotec, Raleigh, NC). The results were obtained with a FLUOstar OPTIMA instrument (BMG Labtech, Offenburg, Germany).

Secretion Assay—Coding sequences for HisRS, HisRSΔCD, and $HisRS^{WHEP}$ were cloned into the pCI-neo-2×myc vector (Promega, Madison, WI) through the NheI/NotI restriction sites. These constructs were transfected into HEK293T cells or C2C12 myoblasts using Lipofectamine LTX with Plus™ reagents (Invitrogen) following the manufacturer's instructions. To achieve similar overexpression levels, the DNA construct of HisRSΔCD or $HisRS^{WHEP}$ was transfected at 1 μg for 2.8×10^5 cells, whereas that of HisRS was transfected at 0.1 μg. Empty vector was transfected as a control. The transfected cells were split when confluent and plated at 2×10^4 cells/cm^2 in a 60-mm dish. Media were refreshed after 3 h, and both media and TCLs were harvested after another 24 h of incubation. The media were precleaned with 5 μl of Dynabeads-protein G (Invitrogen) for 1 h at 4 °C. Anti-Myc polyclonal Ab (1.5 μg; Sigma) was mixed with 5 μl of Dynabeads-protein G in PBS for 1 h at room temperature. The Ab/bead mixture was added to the precleaned media and further incubated for 2 h at 4 °C. The protein-Ab-bead complex was washed with radioimmune precipitation assay buffer (12) and eluted with 0.1 M glycine buffer (pH 2.0). The eluent was neutralized by adding 1 M Tris-HCl (pH 8.0; v/v, 10:1). TCLs were prepared in radioimmune pre-

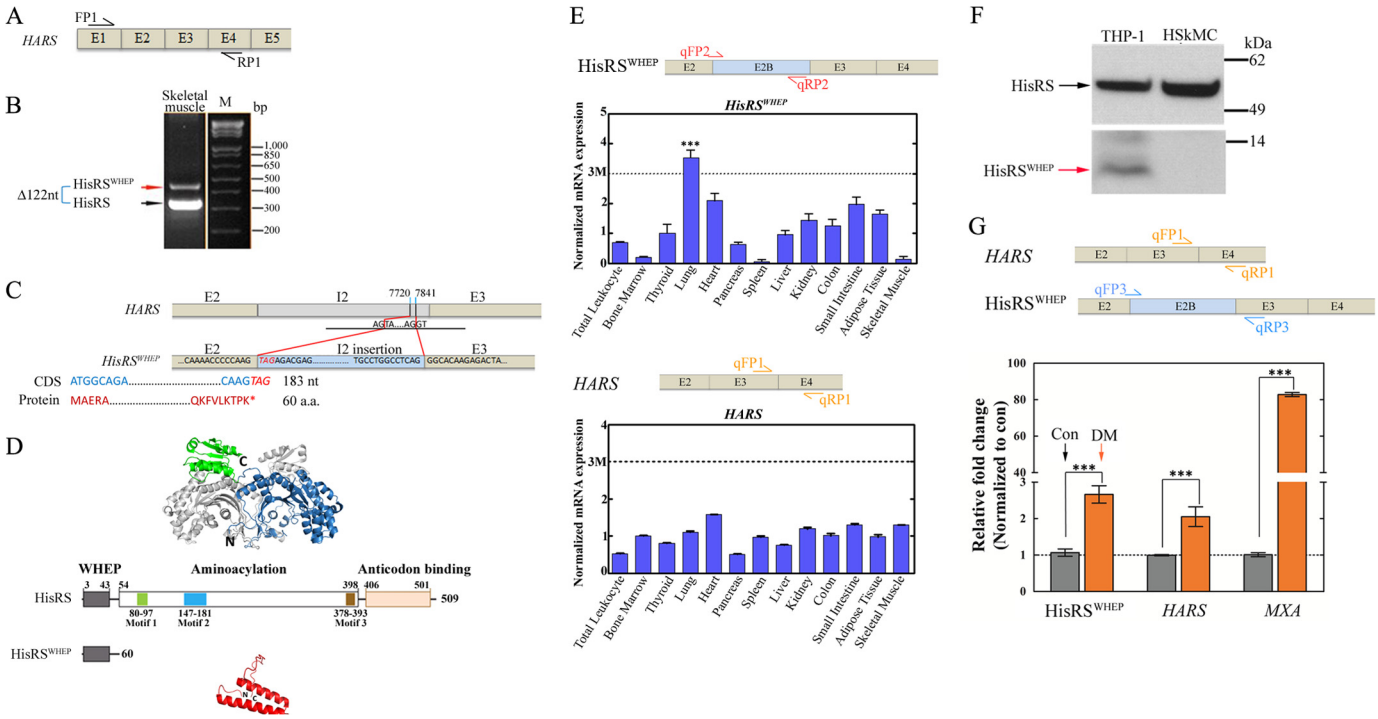

FIGURE 1. **Identification of transcript and protein for HisRS^{WHEP} SV and up-regulation of HisRS^{WHEP} transcript in muscle biopsies of DM patients.** *A*, PCR was used to identify the mRNA encoding HisRS^{WHEP} in human skeletal muscle. Locations of the primers used for PCR are indicated in the schematic. *E*, exon. *B*, electrophoretic analysis of the PCR. The upper fragment (*red arrow*) was amplified from the mRNA for HisRS^{WHEP}, which is 122 nucleotides (*nt*) longer than the lower fragment amplified from the mRNA for *HARS* (*black arrow*). *M*, mass marker. *C*, schematic drawing of the intron 2 (*I2*) insertion in the mRNA for HisRS^{WHEP} and location of the inserted nucleotides in *HARS*. Notably, the inserted sequence is flanked by canonical splicing signals (preceded by AG and followed by GT) and itself ends with AG. HisRS^{WHEP} is encoded by 183 nucleotides and is translated into 60 aa, which encompass the WHEP domain of HisRS. *CDS*, coding sequence. *D*, schematic illustrations of HisRS and HisRS^{WHEP} and their structures (Protein Data Bank code 4G84 for HisRS and code 1X59 for HisRS^{WHEP}). One monomer of HisRS is shown in color (ABD in *green* and CD in *blue*), whereas the other monomer is shown in *gray*. Notably, HisRS^{WHEP} is composed of the N-terminal WHEP domain (shown in *red*) of human *HARS*. *E*, distribution of the transcripts of HisRS and HisRS^{WHEP} in 13 human tissues. Locations of the qPCR primers are indicated in the schematic. The expression levels were normalized to that of the HKG *RPL9*. The median value was taken as 1.0. Notably, the HisRS^{WHEP} transcript is significantly higher in human lung compare with other tissues and is 3-fold above the median. The expression of the transcript for *HARS* was normally distributed in the various tissues, with expression levels <3 times that of the median value. *F*, HisRS^{WHEP} protein was detected in the TCL of monocytic THP-1 cells, but not in that of human skeletal muscle cells (*HSkMC*). Expected running positions of the proteins are indicated by *arrows*. *G*, the transcript for HisRS^{WHEP} is up-regulated in DM muscle biopsies (1.0 $\pm$ 0.1 in control (*Con*) *versus* 2.7 $\pm$ 0.2 in DM). The transcript for HisRS is also up-regulated in the DM samples (1.0 $\pm$ 0.01 in control *versus* 2.1 $\pm$ 0.3 in DM). The *MXA* gene serves as a positive control (1.0 $\pm$ 0.06 in control *versus* 82.8 $\pm$ 1.1 in DM). Locations of the qPCR primers are indicated in the schematic. Data are shown as means $\pm$ S.D. ***, $p < 0.0001$.

cipitation assay buffer (supplemented with protease inhibitors, Roche Applied Science). Both media and TCLs were subjected to electrophoresis and immunoblotted with anti-Myc mAb (Millipore). Lactate dehydrogenase (LDH) protein was detected with anti-LDHB mAb (Abnova).

Cell injury was assessed by measuring LDH activity in the medium (Roche Applied Science). A LDH activity standard was also conducted, covering 0, 25, 50, 100, 200, 400, and 800 microunits/100 μl. The detection limit of the assay was defined as the mean absorbance of the blank plus 3 times the standard deviation of the blank.

RESULTS

Identification of HisRS^{WHEP}—Human HisRS is a class II tRNA synthetase composed of a core CD made up of a seven-stranded β-structure with flanking α-helices and a C-terminal ABD. Although absent from prokaryotic and lower eukaryotic HisRSs, an N-terminal coiled-coil WHEP domain was appended at the time of appearance of metazoans. As stated above, this domain is present in our previously identified HisRSΔCD SV. Our goal was to find additional SVs that retained the WHEP domain.

We noted an expressed sequence tag (EST) BP267368 annotation in the University of California Santa Cruz EST database (13). This transcript has a 122-bp insertion of nucleotides from intron 2, located between exons 2 and 3 (supplemental Fig. S1*A*). Because the intron insertion introduces a stop codon immediately at the end of exon 2, it could, in principle, encode just the WHEP domain of HisRS. To verify this variant, we designed primers that targeted the exon 1 and exon 4 regions of human *HARS* (Fig. 1*A*). PCR with a muscle cDNA template and the aforementioned pair of primers yielded a product of 473 nucleotides, which is larger than that expected for the 351-nucleotide transcript that would encode the same region of full-length *HARS* (Fig. 1*B*). This product confirmed features of the EST BP267368 annotation. However, in contrast to EST BP267368, our SV had neither a T-to-C substitution in exon 2, which would yield a L56P substitution in *HARS*, nor a synonymous A-to-G substitution in exon 3 (supplemental Fig. S1, *B* and *C*). In addition, our analysis differed in having a synonymous T-to-A substitution in the sequence of the insertion into intron 2. The inserted sequence was flanked by consensus GT-AG splice junctions (Fig. 1*C*) and created a new exon cassette. We designated this cassette as exon 2B. The transcript

that results from this splice event harbors a canonical start codon, so translation would start at the typical initiator ATG and terminate after exon 2 (Fig. 1*C*). The consequence is a protein composed of solely the first 60 aa of human HisRS. Because this protein is made up of only the WHEP domain, we named it HisRS^{WHEP} (Fig. 1, *C* and *D*).

Expression of Transcripts for HisRS^{WHEP} in 13 Human Tissue Types—We next compared the transcript levels of HisRS^{WHEP} and *HARS* in 13 human tissue types, which were total leukocytes, bone marrow, spleen, lung, heart, kidney, liver, pancreas, small intestine, colon, thyroid, adipose, and skeletal muscle. The SYBR Green qPCR method was employed. The transcript for *HARS* was somewhat evenly distributed across all 13 tissue types, deviating no more than 3 times from the median value (Fig. 1*E*). (Because the transcript for the housekeeping gene (HKG) *RPL9* (60 S ribosomal protein L9) is the most evenly distributed among ~20 HKGs, the levels of the *HARS* transcripts were normalized to that for *RPL9*.) In comparison, the transcript level of HisRS^{WHEP} was highest in lung (3.5 times above the median level) (Fig. 1*E*). The transcript levels of HisRS^{WHEP} were below 0.1% of those of *HARS*. Interestingly, the expression level of HisRS^{WHEP} was low in normal skeletal muscle tissue in comparison with other tissues.

Detection of HisRS^{WHEP} Protein—We used a standard Western blot method to search for the translation product of the HisRS^{WHEP} transcript. For this purpose, a mAb raised against the N-terminal region (aa 1–97) of human HisRS was used. Considering the relatively small amounts of HisRS^{WHEP} mRNA and the difficulty in obtaining adequate amounts of human tissues, human cell lines cultured *in vitro* were employed. Although not detected in human skeletal muscle cells, the 6.8-kDa HisRS^{WHEP} protein was readily observed in human monocytic THP-1 cells (Fig. 1*F*, *red arrow*). Consistent with the relatively low amount of its mRNA, HisRS^{WHEP} was present at a level estimated close to 1% of that of HisRS, which was detected with the same Ab (Fig. 1*F*, *black arrow*). We also determined the cellular HisRS level in monocytic THP-1 cells by standard sandwich ELISA (see "Experimental Procedures"). Our results show that the intracellular HisRS level was 0.94 ± 0.17 μM (mean ± S.E., $n = 4$).

HisRS^{WHEP} Transcript Is Up-regulated in Pool of Muscle Biopsies from DM Patients—Anti-Jo-1 Abs are present in 15–30% of polymyositis patients and 5–10% of DM patients (14). To evaluate the possibility of HisRS^{WHEP} being an antigen in muscle biopsies of patients with IIM/ILD, we examined its mRNA transcript in pooled muscle biopsies from 10 DM patients. (Because of difficulties in defining primers that were sufficiently specific, the transcript for HisRSΔCD was not measured.) Because *MXA* (myxovirus resistance gene, a type 1 interferon (α/β)) was reported to be up-regulated in myositis (15), its transcript was included as a positive control. Two HKGs, *RPL9* and *RPS11* (40 S ribosomal protein S11), were also included in our analysis. As a control, we used total RNA from two healthy Caucasian subjects. Relative to the control, the transcript for HisRS^{WHEP} was significantly up-regulated in RNA samples from DM muscle biopsies (2.7 ± 0.2-fold, $p < 0.0001$) (Fig. 1*G*). The transcript for native *HARS* was also up-regulated (2.1 ± 0.3-fold, $p < 0.0001$) (Fig. 1*G*).

Anti-Jo-1 Autoantibodies React Mainly with WHEP and ABD Domains of Human HisRS—The N-terminal portion of HisRS, which includes the WHEP domain, has long been recognized as a major epitope of anti-Jo-1 Abs (6, 7). Considering this point, we focused on the antigenicity of two SVs that harbor the WHEP domain, *i.e.* HisRS^{WHEP} and HisRSΔCD. We also investigated recombinant forms of HisRS, CD, and ABD. Recombinant versions of each of these five proteins were expressed in *E. coli* and readily purified. (Thus, all five proteins folded into stable structures.) Depletion ELISAs were used to measure the binding ability of anti-Jo-1 Abs for each of the five proteins (Fig. 2*A*). Sera from 24 anti-Jo-1 Ab-positive patients were included in our analysis. As expected, full-length HisRS almost completely depleted the anti-Jo-1 Abs (~100%) in all patient sera ($n = 24$) (Fig. 2*B*). Strikingly, the CD and ABD recombinant proteins depleted little of the anti-Jo-1 Ab-positive sera. In contrast, ~50% of the anti-Jo-1 Abs reacted with HisRS^{WHEP} and WHEP domain-containing HisRSΔCD. Thus, the two SVs are robust targets for anti-Jo-1 Abs. It is of interest that the domains harbored by these two SVs, the WHEP and ABD domains, are well separated on the structure of native HisRS (Fig. 2, *C* and *D*).

Recombinant HisRS, HisRSΔCD, and HisRS^{WHEP} Are Secreted When Overexpressed in HEK293T Cells—Several examples of secreted human aaRSs have been reported (16–18). Thus, we imagined that, at least as a formal possibility, HisRS and one or both of its SVs could also be secreted under certain conditions, such as in an inflammatory environment. Because our sensitivity of detection was limited by the low abundance of the endogenous splice variants (see above and Ref. 9), as a first step toward investigating secretion, we transiently expressed recombinant HisRS, HisRS^{WHEP}, and HisRSΔCD in HEK293T cells (Fig. 2*E*) and detected their expression by anti-Myc mAb in the TCLs. (The use of the Myc tag enabled us to distinguish the recombinant proteins from endogenous counterparts.) LDHB Western blotting in TCLs served as a loading control. To check for cell leakiness, we measured medium LDH activity using a cytotoxicity kit (19, 20). As shown in the *bar graph* in Fig. 2*E*, all samples had undetectable LDH activity, below the detection limit (indicated by the *dashed red line*), thus suggesting limited (if any) cell damage. Each of the three HisRS proteins was detected in the cell media fraction (Fig. 2*E*). These results support the idea that HisRS, HisRS^{WHEP}, and HisRSΔCD can be secreted into the medium.

Recombinant HisRSΔCD and HisRS Are Secreted When Expressed in C2C12 Myoblasts—We also transiently expressed Myc-tagged recombinant HisRS and HisRSΔCD in C2C12 myoblasts. Both HisRS proteins were expressed in C2C12 myoblasts and detected in the cell media (Fig. 2*F*). LDHB Western blotting in TCLs served as a loading control. (In additional experiments, we could not show that the small WHEP domain alone (HisRS^{WHEP}) could be consistently detected in the media fraction (data not shown), possibly because of variables beyond our immediate control (such as proteases in the media that quickly degrade, like a short polypeptide).) Again, all samples had undetectable LDH activity levels (Fig. 2*F*). These results suggest the possibility that at least one HisRS SV (HisRSΔCD) can be secreted from a murine muscle cell line.

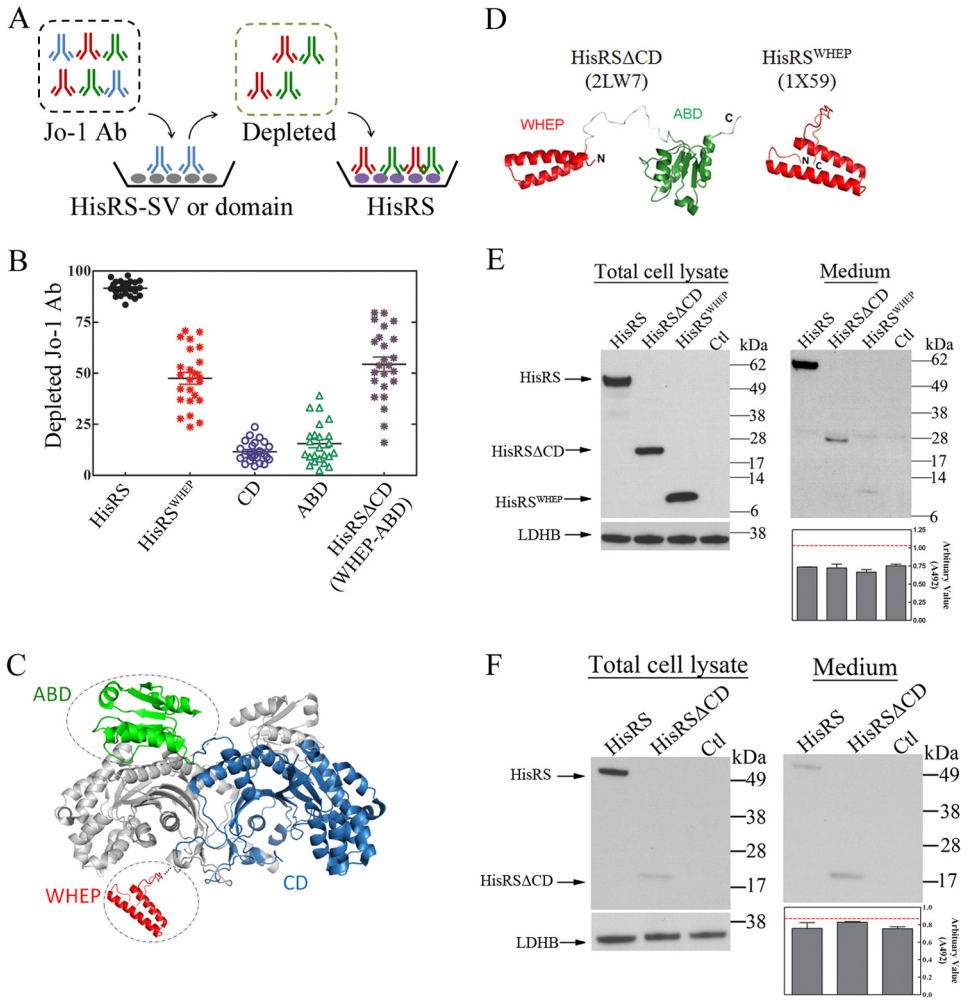

FIGURE 2. **Anti-Jo-1 patient serum reacts mainly with the N-terminal WHEP domain and C-terminal ABD of human HisRS, and recombinant HisRS SVs are secreted from HEK293T cells and C2C12 myoblasts.** *A*, illustration of depletion ELISAs. Details are provided under "Experimental Procedures." *B*, reactivity of anti-Jo-1 Ab-positive patient serum against different HisRS recombinant proteins. Notably, apart from HisRS, anti-Jo-1 Ab-positive patient serum reacted mostly with HisRS^{WHEP} and HisRSΔCD, with a significantly higher reactivity than with the recombinant CD or ABD. *C*, the two most reactive domains are far apart on the three-dimensional structure of HisRS (Protein Data Bank code 4G84). The C-terminal ABD (shown in *green*) and N-terminal WHEP domain (shown in *red*) are highlighted in the structure of HisRS. The N-terminal WHEP domain is not resolved in the structure of HisRS, but is resolved in that of HisRSΔCD (Protein Data Bank code 2LW7). *D*, the structures of HisRSΔCD and HisRS^{WHEP} show that the two HisRS SVs contain the major anti-Jo-1 epitopes. *E* and *F*, recombinant HisRS^{WHEP}, HisRSΔCD, and HisRS proteins (with a C-terminal Myc tag) were transiently expressed in HEK293T cells (*E*), and recombinant HisRSΔCD and HisRS proteins were transiently expressed in C2C12 myoblasts (*F*). Expressed proteins were detected in the TCLs with anti-Myc mAb. LDHB in the TCLs served as a loading control. The media were immunoprecipitated by anti-Myc polyclonal Ab and detected with anti-Myc mAb. Notably, all HisRS proteins were detected in the media. The *bar graphs* show that the LDH activities of all samples were below the detection limit of the assay (indicated by the *red line*), suggesting little cell damage. The results shown are representative of three separately conducted experiments.

DISCUSSION

Several previous studies suggest that low-abundant transcripts, which were previously considered as unimportant, are biologically significant in differentiation, metabolism, and phenotypic alternation (21–25). To better understand the expression of HisRS^{WHEP}, we measured the concentration of human HisRS in monocytic THP-1 cells and showed that intracellular HisRS has a concentration of 0.94 ± 0.17 μM (see above), which is roughly comparable with the reported concentration of methionyl-tRNA synthetase in rabbit reticulocytes (~0.2 μM) (26). On the basis of our estimation that the HisRS^{WHEP} protein is close to 1% of full-length HisRS, we estimate that the cellular content of HisRS^{WHEP} is ~10 nM. Even if only a fraction is secreted, this concentration is well within the range of known dissociation constants (K_d) for aaRSs in cell signaling events. For example, the aaRS complex-interacting multifunctional protein 1 is reported to bind to CD23 with a K_d of 4.3 nM (27); glycyl-tRNA synthetase binds to CDH6 with a K_d of 3.4 nM (16); and a fragment of tyrosyl-tRNA synthetase, known as mini-tyrosyl-tRNA synthetase, stimulates polymorphonuclear cell migration at 1 nM (28). In addition, these concentrations are higher than the effective concentrations of many cytokines, which are in the picomolar to lower nanomolar range. Thus, in healthy young people (<45 years of age), the serum TNF-α level is estimated to be ~0.19 pM, IL-6 is estimated to be ~0.16 pM, and MCP-1 is estimated to be ~16.4 pM (29). From this perspective, our results harmonize well with what is known about many other systems.

Novel functions for the WHEP domains in tryptophanyl-tRNA synthetase, glutamylprolyl-tRNA synthetase, and glycyl-tRNA synthetase have been reported previously (30–34). Interestingly, the WHEP domain-containing N-terminal 48-aa

fragment of HisRS was previously associated with a novel inflammatory function, whereas the residual protein lacking this fragment was inactive (8). Here, we established that two HisRS SVs, unknown at the time of the work of Howard *et al.* (8) and which each harbor the WHEP domain, are expressed in cultured cells and cross-react with a substantial portion of the anti-Jo-1 Abs from the tested patient population. Both SVs and HisRS can also be secreted. In addition, in a DM patient population pool undiagnosed as to anti-Jo-1 Ab status, expression of HisRS and at least one of these SVs appears to be up-regulated (Fig. 1*G*).

Non-translational functions for SVs, natural proteolytic fragments, and even a truncated bipartite synthetase (from the recruitment of a novel stop codon) have been reported for various human tRNA synthetases or synthetase-associated proteins (31, 35–43). These non-translational functions reach into many parts of cell biology and homeostatic mechanisms, including angiogenesis, hematopoiesis, and control of tumor growth. In addition, some of these functions are extracellular and are enabled by the capacity of at least some aaRSs to be secreted, as evidenced by their detection in human and mouse sera (16, 17, 44–47). With this in mind, there are suggestions of immunomodulation-related functions, such that aaRSs fragments have activities that can act to resolve inflammation (48, 49). Thus, in light of the many examples of non-catalytic fragments of aaRSs having extracellular functions and given the data presented here showing the reactivity of SVs of HisRS for anti-Jo-1 Abs, the up-regulation of at least one of them in a patient population, and their secretion from cultured cells, we propose that these SVs deserve further investigations related to muscle health and the etiology of inflammatory muscle diseases.

Possibly, HisRS and its two WHEP domain-containing SVs are involved in maintaining immune homeostasis in muscle. When immune surveillance or clearance is needed, HisRS proteins attract immune cells to muscle tissue. In support of this hypothesis, the N-terminal WHEP domain of HisRS may be chemotactic for lymphocytes and activated monocytes (8). Possibly because of their persistent presence, in DM patients, the HisRS proteins are eventually seen as "foreigners," and autoantibodies against HisRS, especially the WHEP domain, are generated. These autoantibodies may antagonize the immune homeostatic role of HisRS proteins and gradually lead to myositis.

Acknowledgment—We thank the Telethon Network of Genetic Biobanks for kindly providing human DM muscle biopsies.

REFERENCES

1. Love, L. A., Leff, R. L., Fraser, D. D., Targoff, I. N., Dalakas, M., Plotz, P. H., and Miller, F. W. (1991) A new approach to the classification of idiopathic inflammatory myopathy: myositis-specific autoantibodies define useful homogeneous patient groups. *Medicine* **70,** 360–374
2. Targoff, I. N. (2000) Update on myositis-specific and myositis-associated autoantibodies. *Curr. Opin. Rheumatol.* **12,** 475–481
3. Mammen, A. L. (2011) Autoimmune myopathies: autoantibodies, phenotypes and pathogenesis. *Nat. Rev. Neurol.* **7,** 343–354
4. Nishikai, M., and Reichlin, M. (1980) Heterogeneity of precipitating antibodies in polymyositis and dermatomyositis. Characterization of the Jo-1 antibody system. *Arthritis Rheum.* **23,** 881–888
5. Mathews, M. B., and Bernstein, R. M. (1983) Myositis autoantibody inhibits histidyl-tRNA synthetase: a model for autoimmunity. *Nature* **304,** 177–179
6. Martin, A., Shulman, M. J., and Tsui, F. W. (1995) Epitope studies indicate that histidyl-tRNA synthetase is a stimulating antigen in idiopathic myositis. *FASEB J.* **9,** 1226–1233
7. Raben, N., Nichols, R., Dohlman, J., McPhie, P., Sridhar, V., Hyde, C., Leff, R., and Plotz, P. (1994) A motif in human histidyl-tRNA synthetase which is shared among several aminoacyl-tRNA synthetases is a coiled-coil that is essential for enzymatic activity and contains the major autoantigenic epitope. *J. Biol. Chem.* **269,** 24277–24283
8. Howard, O. M., Dong, H. F., Yang, D., Raben, N., Nagaraju, K., Rosen, A., Casciola-Rosen, L., Härtlein, M., Kron, M., Yang, D., Yiadom, K., Dwivedi, S., Plotz, P. H., and Oppenheim, J. J. (2002) Histidyl-tRNA synthetase and asparaginyl-tRNA synthetase, autoantigens in myositis, activate chemokine receptors on T lymphocytes and immature dendritic cells. *J. Exp. Med.* **196,** 781–791
9. Xu, Z., Wei, Z., Zhou, J. J., Ye, F., Lo, W. S., Wang, F., Lau, C. F., Wu, J., Nangle, L. A., Chiang, K. P., Yang, X. L., Zhang, M., and Schimmel, P. (2012) Internally deleted human tRNA synthetase suggests evolutionary pressure for repurposing. *Structure* **20,** 1470–1477
10. Soejima, M., Kang, E. H., Gu, X., Katsumata, Y., Clemens, P. R., and Ascherman, D. P. (2011) Role of innate immunity in a murine model of histidyl-transfer RNA synthetase (Jo-1)-mediated myositis. *Arthritis Rheum.* **63,** 479–487
11. Wang, F., Xu, Z., Zhou, J., Lo, W. S., Lau, C. F., Nangle, L. A., Yang, X. L., Zhang, M., and Schimmel, P. (2013) Regulated capture by exosomes of mRNAs for cytoplasmic tRNA synthetases. *J. Biol. Chem.* **288,** 29223–29228
12. Harlow, E., and Land, David (1999) *Using Antibodies: A Laboratory Manual*, p. 449, Cold Spring Harbor Laboratory Press, Cold Spring Harbor, NY
13. Suzuki, Y., Yamashita, R., Shirota, M., Sakakibara, Y., Chiba, J., Mizushima-Sugano, J., Nakai, K., and Sugano, S. (2004) Sequence comparison of human and mouse genes reveals a homologous block structure in the promoter regions. *Genome Res.* **14,** 1711–1718
14. Jura, M., Rychlewski, L., and Barciszewski, J. (2007) Comprehensive insight into human aminoacyl-tRNA synthetases as autoantigens in idiopathic inflammatory myopathies. *Crit. Rev. Immunol.* **27,** 559–572
15. Greenberg, S. A., Pinkus, J. L., Pinkus, G. S., Burleson, T., Sanoudou, D., Tawil, R., Barohn, R. J., Saperstein, D. S., Briemberg, H. R., Ericsson, M., Park, P., and Amato, A. A. (2005) Interferon-α/β-mediated innate immune mechanisms in dermatomyositis. *Ann. Neurol.* **57,** 664–678
16. Park, M. C., Kang, T., Jin, D., Han, J. M., Kim, S. B., Park, Y. J., Cho, K., Park, Y. W., Guo, M., He, W., Yang, X. L., Schimmel, P., and Kim, S. (2012) Secreted human glycyl-tRNA synthetase implicated in defense against ERK-activated tumorigenesis. *Proc. Natl. Acad. Sci. U.S.A.* **109,** E640–E647
17. Kapoor, M., Zhou, Q., Otero, F., Myers, C. A., Bates, A., Belani, R., Liu, J., Luo, J. K., Tzima, E., Zhang, D. E., Yang, X. L., and Schimmel, P. (2008) Evidence for annexin II-S100A10 complex and plasmin in mobilization of cytokine activity of human TrpRS. *J. Biol. Chem.* **283,** 2070–2077
18. Wakasugi, K., and Schimmel, P. (1999) Two distinct cytokines released from a human aminoacyl-tRNA synthetase. *Science* **284,** 147–151
19. Rouabhia, M., Park, H., Meng, S., Derbali, H., and Zhang, Z. (2013) Electrical stimulation promotes wound healing by enhancing dermal fibroblast activity and promoting myofibroblast transdifferentiation. *PLoS ONE* **8,** e71660
20. Chan, F. K. M., Moriwaki, K., and De Rosa, M. J. (2013) Detection of necrosis by release of lactate dehydrogenase activity. *Methods Mol. Biol.* **979,** 65–70
21. Elowitz, M. B. (2002) Stochastic gene expression in a single cell. *Science* **297,** 1183–1186
22. Kuznetsov, V. A., Knott, G. D., and Bonner, R. F. (2002) General statistics of stochastic process of gene expression in eukaryotic cells. *Genetics* **161,** 1321–1332
23. Ozbudak, E. M., Thattai, M., Kurtser, I., Grossman, A. D., and van Oudenaarden, A. (2002) Regulation of noise in the expression of a single gene.

Nat. Genet. **31,** 69–73
24. Blake, W. J., KAErn M., Cantor, C. R., and Collins, J. J. (2003) Noise in eukaryotic gene expression. *Nature* **422,** 633–637
25. Paulsson, J. (2004) Summing up the noise in gene networks. *Nature* **427,** 415–418
26. Kellermann, O., Tonetti, H., Brevet, A., Mirande, M., Pailliez, J. P., and Waller, J. P. (1982) Macromolecular complexes from sheep and rabbit containing seven aminoacyl-tRNA synthetases. I. Species specificity of the polypeptide composition. *J. Biol. Chem.* **257,** 11041–11048
27. Kwon, H. S., Park, M. C., Kim, D. G., Cho, K., Park, Y. W., Han, J. M., and Kim, S. (2012) Identification of CD23 as a functional receptor for the proinflammatory cytokine AIMP1/p43. *J. Cell Sci.* **125,** 4620–4629
28. Vo, M. N., Yang, X. L., and Schimmel, P. (2011) Dissociating quaternary structure regulates cell-signaling functions of a secreted human tRNA synthetase. *J. Biol. Chem.* **286,** 11563–11568
29. Kim, H., Kim, H. S., Youn, J. C., Shin, E. C., and Park, S. (2011) Serum cytokine profiles in healthy young and elderly population assessed using multiplexed bead-based immunoassays. *J. Transl. Med.* **9,** 113
30. Wakasugi, K., Slike, B. M., Hood, J., Otani, A., Ewalt, K. L., Friedlander, M., Cheresh, D. A., and Schimmel, P. (2002) A human aminoacyl-tRNA synthetase as a regulator of angiogenesis. *Proc. Natl. Acad. Sci. U.S.A.* **99,** 173–177
31. Zhou, Q., Kapoor, M., Guo, M., Belani, R., Xu, X., Kiosses, W. B., Hanan, M., Park, C., Armour, E., Do, M. H., Nangle, L. A., Schimmel, P., and Yang, X. L. (2009) Orthogonal use of a human tRNA synthetase active site to achieve multifunctionality. *Nat. Struct. Mol. Biol.* **17,** 57–61
32. Sajish, M., Zhou, Q., Kishi, S., Valdez, D. M., Jr., Kapoor, M., Guo, M., Lee, S., Kim, S., Yang, X. L., and Schimmel, P. (2012) Trp-tRNA synthetase bridges DNA-PKcs to PARP-1 to link IFN-γ and p53 signaling. *Nat. Chem. Biol.* **8,** 547–554
33. He, W., Zhang, H. M., Chong, Y. E., Guo, M., Marshall, A. G., and Yang, X. L. (2011) Dispersed disease-causing neomorphic mutations on a single protein promote the same localized conformational opening. *Proc. Natl. Acad. Sci. U.S.A.* **108,** 12307–12312
34. Jia, J., Arif, A., Ray, P. S., and Fox, P. L. (2008) WHEP domains direct non-canonical function of glutamyl-prolyl tRNA synthetase in translational control of gene expression. *Mol. Cell* **29,** 679–690
35. Wu, P. C., Alexander, H. R., Huang, J., Hwu, P., Gnant, M., Berger, A. C., Turner, E., Wilson, O., and Libutti, S. K. (1999) *In vivo* sensitivity of human melanoma to tumor necrosis factor (TNF)-α is determined by tumor production of the novel cytokine endothelial-monocyte activating polypeptide II (EMAPII). *Cancer Res.* **59,** 205–212
36. Shalak, V. (2001) The EMAPII cytokine is released from the mammalian multisynthetase complex after cleavage of its p43/proEMAPII component. *J. Biol. Chem.* **276,** 23769–23776
37. Banin, E. (2006) T2-TrpRS inhibits preretinal neovascularization and enhances physiological vascular regrowth in OIR as assessed by a new method of quantification. *Invest. Ophthalmol. Vis. Sci.* **47,** 2125–2134
38. Tzima, E., Reader, J. S., Irani-Tehrani, M., Ewalt, K. L., Schwartz, M. A., and Schimmel, P. (2003) Biologically active fragment of a human tRNA synthetase inhibits fluid shear stress-activated responses of endothelial cells. *Proc. Natl. Acad. Sci. U.S.A.* **100,** 14903–14907
39. Mukhopadhyay, R., Jia, J., Arif, A., Ray, P. S., and Fox, P. L. (2009) The GAIT system: a gatekeeper of inflammatory gene expression. *Trends Biochem. Sci.* **34,** 324–331
40. Han, J. M., Park, B. J., Park, S. G., Oh, Y. S., Choi, S. J., Lee, S. W., Hwang, S. K., Chang, S. H., Cho, M. H., and Kim, S. (2008) AIMP2/p38, the scaffold for the multi-tRNA synthetase complex, responds to genotoxic stresses via p53. *Proc. Natl. Acad. Sci. U.S.A.* **105,** 11206–11211
41. Choi, J. W., Kim, D. G., Park, M. C., Um, J. Y., Han, J. M., Park, S. G., Choi, E. C., and Kim, S. (2009) AIMP2 promotes TNF-dependent apoptosis via ubiquitin-mediated degradation of TRAF2. *J. Cell Sci.* **122,** 2710–2715
42. Choi, J. W., Lee, J. W., Kim, J. K., Jeon, H. K., Choi, J. J., Kim, D. G., Kim, B. G., Nam, D. H., Kim, H. J., Yun, S. H., and Kim, S. (2012) Splicing variant of AIMP2 as an effective target against chemoresistant ovarian cancer. *J. Mol. Cell Biol.* **4,** 164–173
43. Choi, J. W., Kim, D. G., Lee, A. E., Kim, H. R., Lee, J. Y., Kwon, N. H., Shin, Y. K., Hwang, S. K., Chang, S. H., Cho, M. H., Choi, Y. L., Kim, J., Oh, S. H., Kim, B., Kim, S. Y., Jeon, H. S., Park, J. Y., Kang, H. P., Park, B. J., Han, J. M., and Kim, S. (2011) Cancer-associated splicing variant of tumor suppressor AIMP2/p38: pathological implication in tumorigenesis. *PLoS Genet.* **7,** e1001351
44. Park, S. G., Kim, H. J., Min, Y. H., Choi, E. C., Shin, Y. K., Park, B. J., Lee, S. W., and Kim, S. (2005) Human lysyl-tRNA synthetase is secreted to trigger proinflammatory response. *Proc. Natl. Acad. Sci. U.S.A.* **102,** 6356–6361
45. Williams, T. F., Mirando, A. C., Wilkinson, B., Francklyn, C. S., and Lounsbury, K. M. (2013) Secreted threonyl-tRNA synthetase stimulates endothelial cell migration and angiogenesis. *Sci. Rep.* **3,** 1317
46. Ko, Y. G. (2001) A cofactor of tRNA synthetase, p43, is secreted to up-regulate proinflammatory genes. *J. Biol. Chem.* **276,** 23028–23033
47. Greenberg, Y., King, M., Kiosses, W. B., Ewalt, K., Yang, X., Schimmel, P., Reader, J. S., and Tzima, E. (2008) The novel fragment of tyrosyl-tRNA synthetase, mini-TyrRS, is secreted to induce an angiogenic response in endothelial cells. *FASEB J.* **22,** 1597–1605
48. Kron, M. A., Wang, C., Vodanovic-Jankovic, S., Howard, O. M., and Kuhn, L. A. (2012) Interleukin-8-like activity in a filarial asparaginyl-tRNA synthetase. *Mol. Biochem. Parasitol.* **185,** 66–69
49. Kron, M. A., Metwali, A., Vodanovic-Jankovic, S., and Elliott, D. (2013) Nematode asparaginyl-tRNA synthetase resolves intestinal inflammation in mice with T-cell transfer colitis. *Clin. Vaccine Immunol.* **20,** 276–281